# Experimental Comparison of Cracking in Four Masonry Walls with Different Boundaries and Material

Korswagen, Paul; Gaggero, M. Belen; Rots, Jan G.

**DOI**
10.1007/978-3-031-73310-9_23

**Publication date**
2025

**Document Version**
Final published version

**Published in**
18th International Brick and Block Masonry Conference

**Citation (APA)**
Korswagen, P., Gaggero, M. B., & Rots, J. G. (2025). Experimental Comparison of Cracking in Four Masonry Walls with Different Boundaries and Material. In G. Milani, & B. Ghiassi (Eds.), *18th International Brick and Block Masonry Conference: Proceedings of IB2MaC 2024—Volume 2* (Vol. 2, pp. 322-332). (Lecture Notes in Civil Engineering; Vol. 614). Springer. https://doi.org/10.1007/978-3-031-73310-9_23

# Experimental Comparison of Cracking in Four Masonry Walls with Different Boundaries and Material

Paul Korswagen(✉), M. Belen Gaggero, and Jan G. Rots

Faculty of Civil Engineering and Geosciences, Delft University of Technology, Delft, The Netherlands
p.a.korswageneguren@tudelft.nl

**Abstract.** Within the context of light damage to unreinforced masonry structures, recent tests have shown that the cracking behaviour of calcium-silicate brick masonry walls makes them more vulnerable to in-plane loads when compared against fired-clay brick walls. To further explore this observation, four nominally-identical walls have been tested. Two of the specimens (3m wide and 2.7m tall) were built with calcium-silicate bricks and two with fired-clay bricks. Additionally, two boundaries were compared: a top cantilever boundary, and a doubled-clamped configuration. The quasi-static, in-plane, two-way cyclic tests imposed small (0.03 to 0.1%), repeated drifts on the walls to investigate the initiation and propagation of small cracks. To monitor the cracking behaviour, high resolution Digital Image Correlation was applied. At the end of the tests, large drifts up to 2% were exerted to compare the near-collapse behaviour of the walls.

The tests revealed that the walls with the more restrictive boundary, deforming mostly in shear, behaved the stiffest and also developed cracks earlier than the cantilever walls. Additionally, this constraint also led to more vertical cracks that split bricks, while the cantilever walls saw more horizontal and diagonal cracks along mortar joints and at mortar-brick interfaces. While the calcium-silicate-proved to be more brittle than the fired-clay masonry for the cantilever test, the clay masonry exhibited similar brick-splitting cracks in the double-clamped configuration. In general, there were fewer but wider cracks in the calcium-silicate specimens, while the clay brick samples showed less localisation and more smeared-crack behaviour. In terms of stiffness, the calcium-silicate walls were initially stiffer and achieved a higher capacity. Moreover, these walls also presented a higher hysteresis associated with more frictional failures. In sum, while cracks on the calcium-silicate walls were confirmed to be more serious, their increased stiffness could lead to smaller drifts during dynamic loading, and the walls would develop less damage; this requires further study.

**Keywords:** Masonry · Crack Damage · Laboratory Experiments

## 1 Introduction

The northern regions of the Netherlands experience frequent but relatively minor earthquakes due to natural gas extraction activities, as reported by NAM in 2016. These tremors generate ground vibrations ranging from 2 to 10 mm/s, with the highest recorded


G. Milani and B. Ghiassi (Eds.): IB2MaC 2024, LNCE 614, pp. 322–332, 2025.
https://doi.org/10.1007/978-3-031-73310-9_23

peak ground velocity (PGV) being 32 mm/s, according to den Bezemer and van Elk (2018). Such vibrations can cause minor, or DS1 level, damage to the prevalent unreinforced masonry buildings in the area. Moreover, the Netherlands has an abundance of soft soils on which buildings with shallow foundations are constructed. These leads to settlement damage also in the DS1 or DS2 levels.

Buildings constructed before 1970 typically feature double wythe or cavity walls made of fired-clay bricks. In contrast, buildings erected after 1970 usually have cavity walls with a structural inner layer of calcium-silicate bricks and an exterior layer of clay bricks. This construction method evolved in the 1990s to include larger calcium-silicate blocks or elements.

As a result, many residential buildings now have walls that combine calcium-silicate and fired-clay bricks. Understanding the damage patterns of both types of walls is crucial for predicting the minor damages these structures may sustain due to seismic activities. Initially, this involves comparing the response of each material to similar levels of inter-storey drift, assuming the walls act cohesively at the floor connections. This assumption is valid for minor damages primarily caused by in-plane forces, while out-of-plane forces are more relevant to severe damages, as noted by Van Staalduinen et al. (2018).

This paper presents a comparison through experimental tests on full-scale walls. Building on the work presented at the last conference (Korswagen and Rots 2020), which examined the cracking patterns of fired-clay versus calcium-silicate brick masonry, this study introduces new tests that incorporate a critical boundary condition—a double-clamped configuration with an opening—not previously examined. This advancement enables a more comprehensive comparison and enhances our understanding of the in-plane, crack-induced, minor-damage behaviour of masonry structures.

## 2 Experimental Tests on Full-Scale Walls

### 2.1 Description of the Wall Tests

Four full-scale masonry walls of about 3.1 m wide and 2.7 m tall (see Fig. 1) were tested in-plane. The tests were performed displacement-controlled and considered cyclically increasing lateral drift. Two walls were built of calcium-silicate bricks with a cementitious general mortar in joints of 10 mm. Additionally, two walls of fired-clay brick masonry were constructed and tested in a similar manner (see Table 1). Note that the fired-clay units were 50 mm high white the calcium-silicate units were 70 mm high. An opening for a window, located asymmetrically towards the centre of the wall and covered with a precast concrete lintel, divided the walls in two piers and two spandrels, and would later serve for the initiation of cracks. These four walls join a database of similar walls tested at the Delft University of Technology in the past.

So that clear comparisons could be drawn, the four tests were conducted identically except for the two boundary possibilities. The two walls subjected to the cantilever boundary (one of clay and another of calcium-silicate) were pre-stressed with a vertical overburden of 0.12 MPa. In the cantilever boundary, the top beam was allowed to rotate. The remaining two walls were tested double-clamped or fixed-fixed. In this case, the control system, including four vertical hydraulic actuators in addition to the horizontal actuator used to enforce the drift, was configured such that it would enforce that the

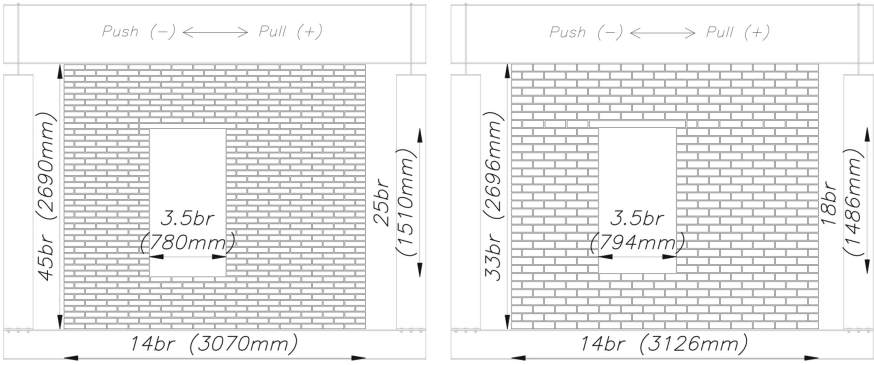


**Fig. 1.** The two types of geometry for fired-clay, left, and calcium-silicate brick, right.

top beam remained parallel to the bottom beam. To maintain this control, the vertical overburden was increased to 0.36 MPa. Because the test of Comp54 was interrupted due to a control error, an earlier wall (TUD-Component 43) is also used for the comparison; fortunately, the double-clamped tests, that were completely new, could be conducted successfully.

**Table 1** Matrix of the four full-scale brick masonry walls.

| Boundary/Material | Fired-Clay | Calcium-Silicate |
|---|---|---|
| Cantilever | TUD-Component 43 / 54 | TUD-Component 52 |
| Double-Clamped | TUD-Component 55 | TUD-Component 53 |

The quasi-static tests started at an enforced drift of 0.26‰ which was increased by a value of 0.073‰ after 30 one-way cycles in the positive direction. This means that 30 cycles were performed at a drift of 0.26‰ in step 1. The drift was increased four times for a total of 5 one-way steps, before it was reduced back to 0.26‰ and the step-wise increasing procedure was repeated for two-way cycles (positive and negative in-plane directions), with a total of 7 additional steps, ultimately reaching a drift of 0.7‰ in the last, twelfth step; for the double-clamped boundary, an initial step with a drift of 0.20‰ was also tested.

Additionally, the specimens are fully utilised by including a test until failure. This is the near-collapse part of the test and corresponds to the ultimate limit state. This protocol includes steps of a single repetition each with drifts of 1‰, 3‰, 5‰, 8‰, 1%, 1.6%, 2.1%, and 3%.

The specimens were painted white and a black pattern of random dots was applied to monitor displacements on the surface of the wall using Digital Image Correlation. Figure 2 presents a photograph of the wall with a corner zoomed-in to show the speckle pattern. The 2D, in-plane displacements of approximately one million gridpoints, spaced about 2.8 mm from each other, were surveyed simultaneously at an accuracy of 20 μm.

The setup was configured so as to track the initiation and propagation of cracks in the masonry; the former was considered to occur when cracks reached a width of 100 μm, as lines of this thickness start to become visible to the naked eye of a careful observer. Additionally, LVDTs and laser sensors at the back of the wall verified in-plane and out-of-plane deformations, respectively.

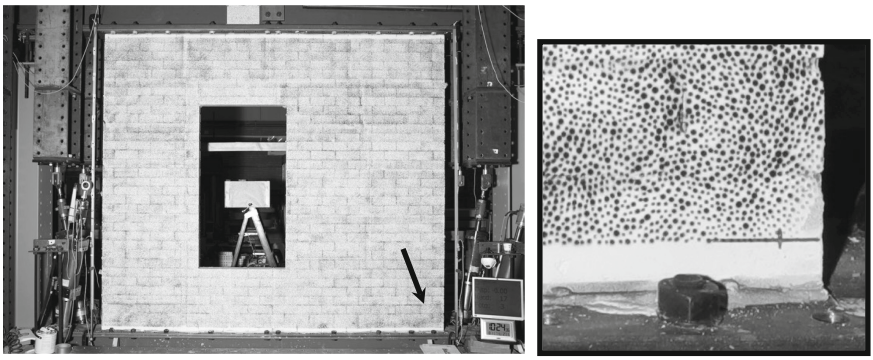

**Fig. 2.** Calcium-silicate brick wall painted white with a black speckle pattern for Digital Image Correlation. Zoom-in of the bottom right corner.

### 2.2 Results of the Wall Tests During Light Damage

The lateral force opposed by the walls when applying the prescribed displacements was recorded. When plotted against the enforced drift, a force-displacement curve can be drawn. Figure 3 compares the four walls for the repetitive part of the protocol (when the drift was applied only in one direction without reversal). The five or six incremental steps are visible. The curves reveal that the doubled-clamped tests reached a higher capacity—this is expected since the overburden was also higher. However, both walls, independent of the material, also achieved noticeable higher forces at each step while the cantilever tests quickly reached their capacity and present a more plastic force-drift envelope. In terms of hysteretic energy, no remarkable differences can be observed for all four walls, while the calcium-silicate walls do show slightly larger energy release.

A similar comparison is conducted for the two-way cyclic protocol that followed. Here, the positive drift direction is already damage and most of the energy release occurs in the negative direction. Indeed, the calcium-silicate walls show a slightly larger release followed by the double-clamped test of the fired-clay wall. At each loading step, the force degradation is very clear for the double-clamped condition: one can observe that at each repetition of the drift, a lower lateral force is required. The force degradation is coupled to a reduced stiffness, meaning that the walls progressively become more flexible.

The force-drift behaviour of the walls could be idealised with a bi-linear diagram. For the cantilever walls, the upper branch would be more horizontal, while the double-clamped walls display a steeper branch. Beyond light-damage, a tri-linear diagram could be used; see next section (Fig. 4).

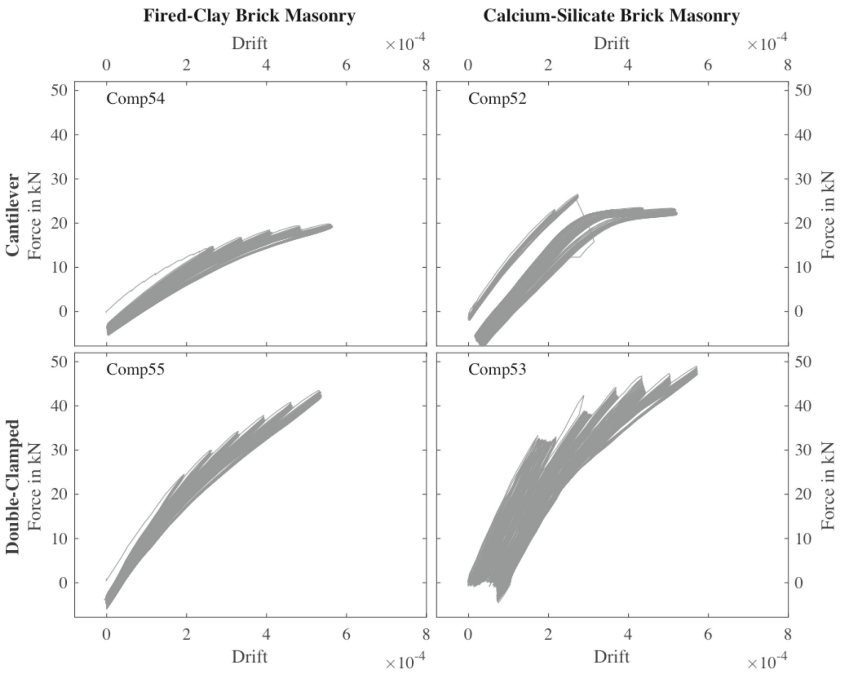


**Fig. 3.** Force-Drift curves for the four walls during the repetitive loading protocol.

At the end of the cyclic protocol, the summative crack pattern is gathered in Fig. 5. Clear differences can be observed for the two materials and the two boundary conditions. For the cantilever cases, cracks appeared more horizontal and followed a somewhat diagonal path. For the fixed-fixed condition, a steeper path is visible. Similarly, the CaSi walls display more diagonal and even vertical paths, cutting through the units. Moreover, the double-clamped cases seem to show more smeared cracks while the cantilever walls display more localised cracks directly propagating from the window corners. Nonetheless, the cracks for the fixed-fixed boundary are consistently wider, but not remarkably so.

### 2.3 Results of the Wall Tests for Near Collapse

The light-damage portion of the protocol reaches drift values up to ±0.7‰, or about 2.1 mm. At this point, the crack patterns are complete and subsequent damage aggravation corresponds only on widening of the existing cracks. On the force-displacement curves, the capacity has been reached but a drop in capacity is not developed. This represents the end of the light-damage behaviour encompassing the serviceability limit states, damage limitation, damage states 1 and 2, etc. The significant damage threshold gives way to higher damage states, including the near-collapse and ultimate-limit state behaviour. During the near-collapse protocols, much higher drift values are achieved, up to ±2%. These are associated with a general loss in capacity and stiffness. Because of this, some tests are culminated earlier when a drop of 20% in capacity was registered. The stability

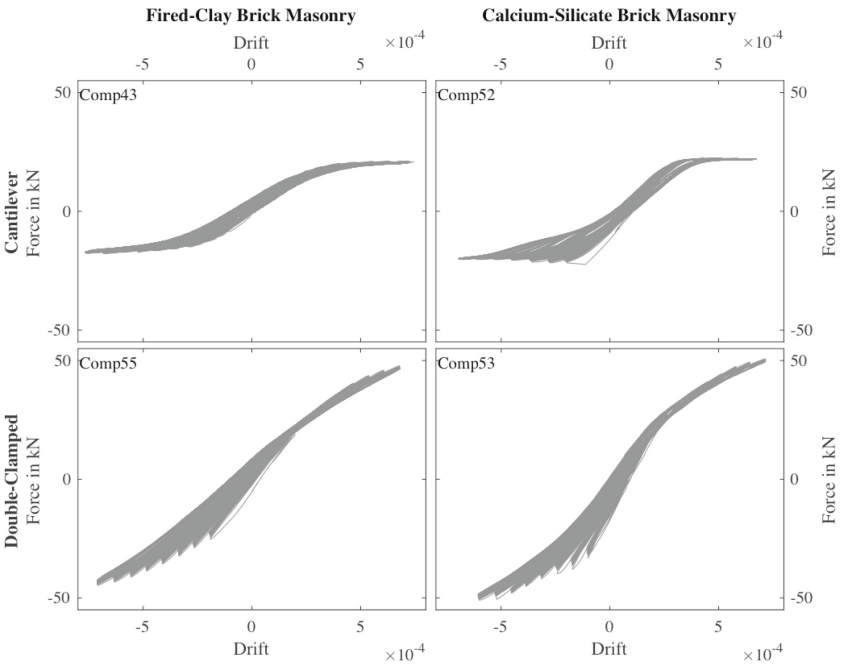


**Fig. 4.** Force-Drift curves for the four walls during the two-way cyclic loading protocol.

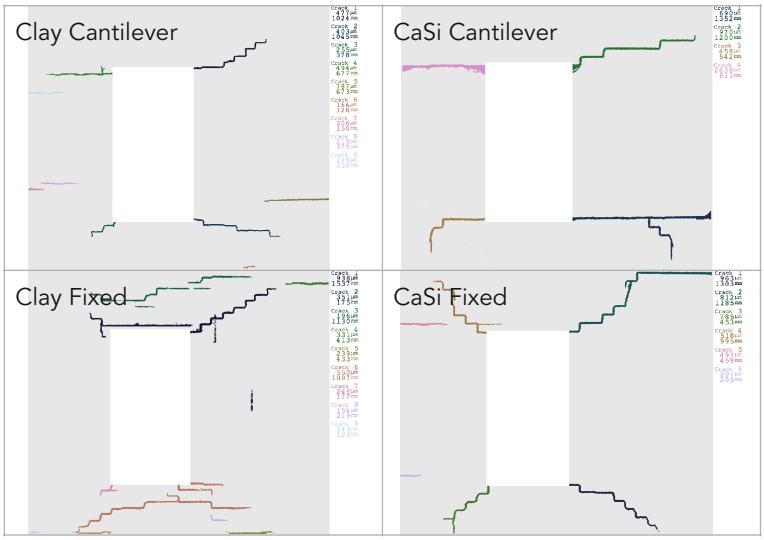


**Fig. 5.** Summative crack pattern at the end of the cyclic protocol.

of the walls in the out-of-plane direction was also monitored and the tests were stopped if continuing was deemed unsafe.

The shape of the force-drift curves are linked to the failure mechanism of each test. In general, pure rocking with crack opening and closing, and pure shear, with only sliding at the crack interface, can be distinguished. The various walls exhibited combinations of these mechanisms at different degrees on the two possible directions. For example, Comp43 displays mostly sliding in both directions; Comp52 in contrast, shows sliding only in the negative drift direction while the positive direction is associated with pure rocking. The other two walls, in doubled-clamped configuration, present a mixed mechanism. The boundary motivates sliding but is also accompanied by Mode I crack opening and closing. For Comp55, the negative direction sees little sliding while Comp53, after clear failures, starts to slide (Fig. 6).

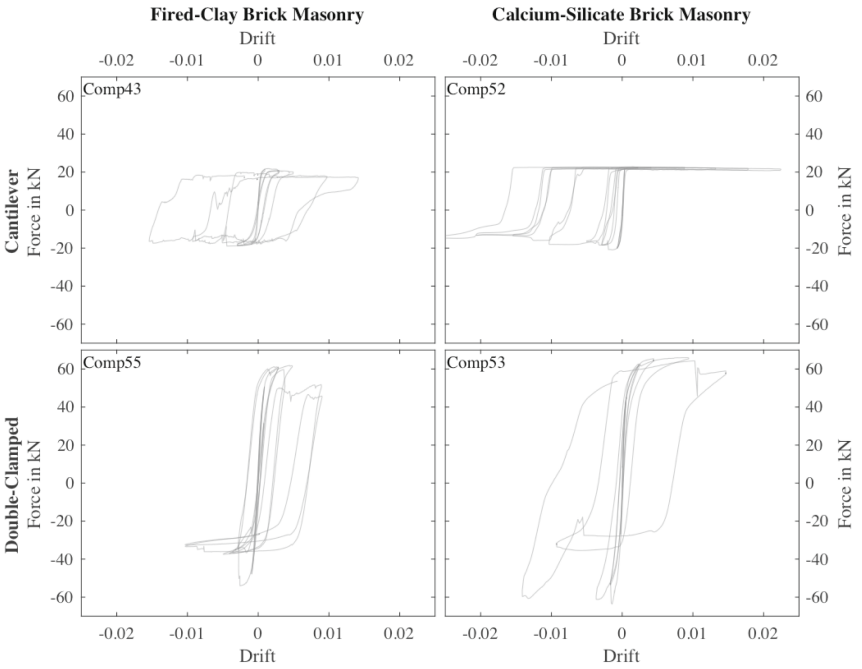


**Fig. 6.** Force-drift curves for the near-collapse protocol.

This can also be inferred from the final crack patterns, presented in Fig. 7, at the end of the tests. Here, the earlier cracks have been aggravated and depict walls that have separated into rigid bodies; these slide or rotate against each other.

## 3 Discussion

The results can be further processed to identify the maximum force and the maximum damage at each step. The lateral force is measured at the actuator and damage is determined with the DIC system. The latter is configured such that an image is captured at precisely the peak of the applied drift, corresponding to each cycle in each step. From

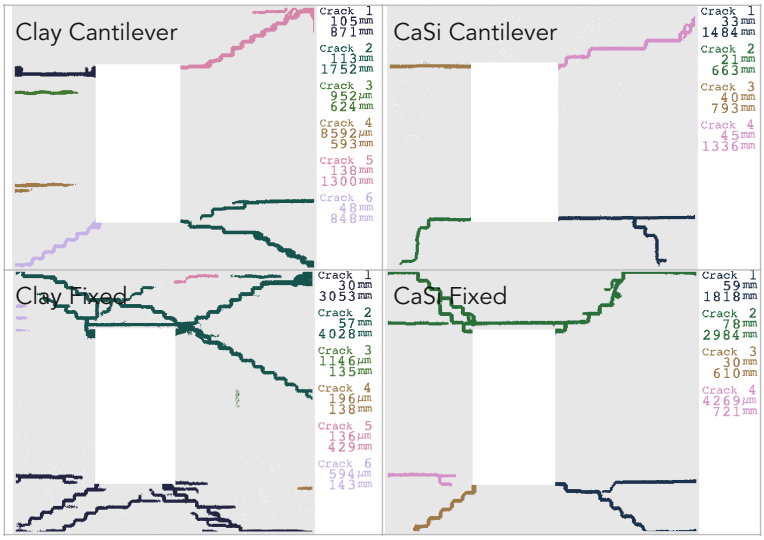


**Fig. 7.** Summative crack pattern at the end of the near-collapse test.

the DIC image, the displacements are employed to determine the location and characteristics of cracks. The cracks are then assembled in the damage parameter Ψ that considers the number, crack width and crack length to compute a scalar intensity (Korswagen and Rots 2020). With Ψ, the damage evolution between the similar walls can be compared throughout the test.

In Fig. 8, the comparison is first conducted in terms of force. The behaviour observed in Figs. 3 and 4 is here emphasised: the cantilever tests display a lower capacity. It is also clear that the fired-clay specimen shows a lower capacity for the cantilever boundary and for the double-clamped tests. The force at each step degrades; in the positive direction, this occurs during the repetitive protocol, while for the cyclic protocol, this occurs only in the negative direction since the positive direction has already been damaged. The degradation is more consistent during the double-clamped tests. A hypothesis is that the predominantly shear behaviour, that follows from this boundary condition, is also linked to the observed reduction in force.

A similar behaviour can be observed if the force is replaced by crack-based damage measured with Ψ as in Fig. 9. Here, one can observe that damage increases as the applied drift increases. While clear increases occur when the drift is changed, this happens even within each step where the applied drift is constant. In particular, towards the end of the protocol, the increase in damage within each step is clear. In the negative direction, measuring Ψ appears noisy, especially for the double-clamped protocol. This might be related to the sensitivity of the DIC system but also suggests that the configuration of the cracks changes during the step. It is possible that progressive sliding—linked to a force degradation—also leads to an alternating picture of cracks that are more and then less open.

In general, all walls exhibit similar damage. Consistently, Comp55, the fired-clay wall under double-clamped condition, shows the least damage. The calcium-silicate

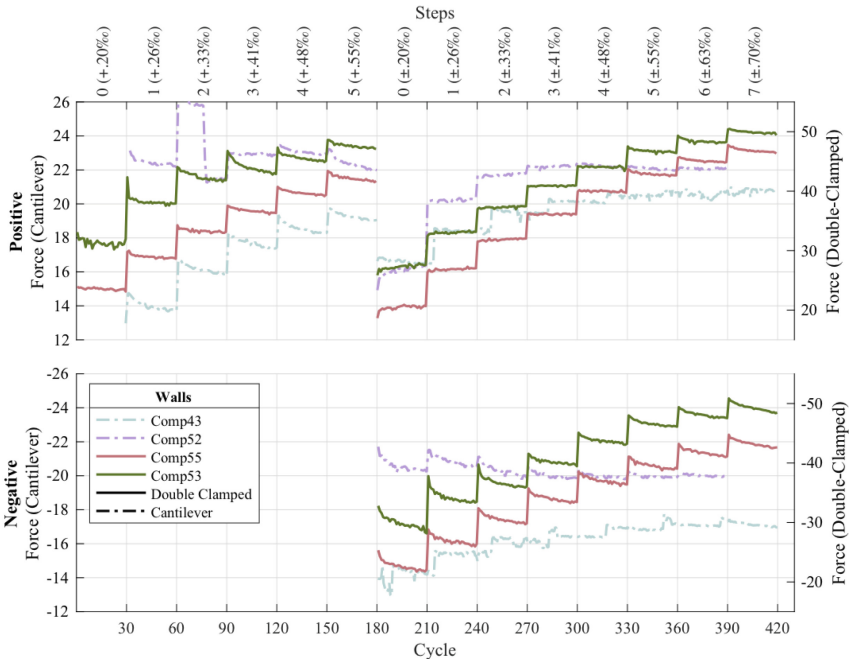


**Fig. 8.** Maximum force reached during each cycle for the positive drift direction, top, and the negative direction, bottom. Fired-clay: Comp43 and 55. Calcium-silicate: Comp52 and 53.

specimen, double-clamped, follows, though is more comparable to the cantilever tests. These two present the most damage, though overall the calcium-silicate specimen gets damaged earlier. Damage ranges from $\Psi = 1$ (just visible cracks) to almost $\Psi = 3$ at the end of the light or minor damage.

The doubled-clamped boundary is associated with a larger overburden. There are two reasons for this. First, in buildings, walls subjected mostly to shear instead of flexure, also bear a higher vertical load. Second, in the experimental setup, the overburden is a result of the required tensile force in the vertical jacks that enforce the double-clamped configuration. The larger overburden of 0.46 against 0.12 MPa, could also have an influence on the results. The stress distribution is more uniform in the shear walls and comprises both shear and compression; for the cantilever walls, rocking produces a localised compressive stress with little shear. From these tests, it is not possible to isolate the effect of the overburden. Additional experiments at different overburdens would be required in order to gather more conclusive observations.

In literature, several tests of masonry walls with openings and a double-clamped boundary can be found. In particular, the campaign of Vermeltfoort (1993) is well known. These smaller walls were tested monotonically in one direction. The crack pattern is very similar to the double-clamped walls tested here, regardless of the material: the cracks propagate diagonally from the opposite window corners. Then, at the tip of crack, the path diverges from the brick-mortar interface and splits the units.

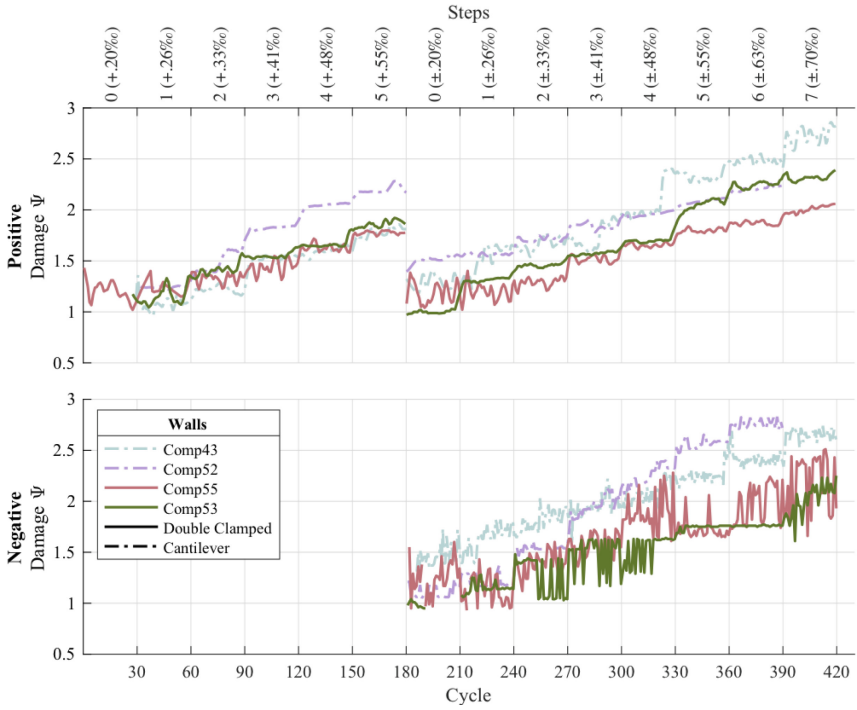


**Fig. 9.** Damage, measured with Ψ, at each step over the repetitive and cyclic protocols.

## 4 Conclusions

Four tests on full-scale masonry walls have been performed. Only the material and the boundary enforced on the walls was changed with the goal of comparing the experiments and assessing the influence of these changes. Moreover, the geometry of the walls, with a window opening placed asymmetrically, had not previously been subjected to a double-clamped configuration, where the top and bottom boundaries are kept parallel, and had only been tested in cantilever form. Fired-clay brick masonry and calcium-silicate brick masonry were compared against each other.

The experiments reveal that the double clamped configuration is more sensitive to an aggravation of damage due to repetitive loading. Similarly, the force required to apply equal values of drift quickly diminishes with each repetition. This effect is also visible in the cantilever tests though it appears stronger during the double-clamped tests. For this effect, the material of the wall seemed not to play a role. However, in terms of damage, the cantilever tests show more intense crack-based damage as do the specimens with the calcium-silicate material.

The lateral capacity of the walls tested in double-clamped configuration is higher but this is also related to the larger overburden applied during these tests. In terms of drift, the cantilever tests could endure a larger drift during near-collapse before the tests were finalised either due to stability concerns or because the capacity had dropped more than 20%.

In sum, these comparative tests are a welcome addition to the database of masonry walls tested at low drifts and surveyed with crack-tracking photogrammetry.

## References

den Bezemer T, van Elk J (2018) Special report on the Zeerijp earthquake. NAM

Del Gaudio C, De Risi MT, Ricci P, Verderame GM (2017) Drift-based fragility functions for hollow clay masonry infills in RC buildings under in-plane seismic actions. Anidis, 2017, Pistoia

Hak S, Morandi P, Magenes G (2017) Verification of drift demands in the design of RC buildings with masonry infills. In: 16th world conference on earthquake engineering. 16WCEE 2017 Santiago Chile

Jafari S, Esposito R, Rots JG, Messali F (2017) Characterizing the material properties of dutch unreinforced masonry. Procedia Eng 193:250–257

Kallioras S, Graziotti F, Penna A (2018) Numerical assessment of the dynamic response of a URM terraced house exposed to induced seismicity. Bull Earthq Eng. https://doi.org/10.1007/s10518-018-0495-5

Korswagen PA, Longo M, Meulman E, Rots JG (2019) Crack initiation and propagation in unreinforced masonry specimens subjected to repeated in-plane loading during light damage. Bull Earthq Eng. https://doi.org/10.1007/s10518-018-00553-5

NAM (2016) Production, Subsidence, Induced Earthquakes and Seismic Hazard and Risk Assessment in the Groningen Field. NAM, Technical Addendum to the Winningsplan Groningen 2016. Downloadable from www.NAM.nl

Van Staalduinen PC, Terwel K, Rots JG (2018) Onderzoek naar de oorzaken van bouwkundige schade in Groningen Methodologie en case studies ter duiding van de oorzaken. Delft University of Technology. Report number CM-2018-01, 11 July 2018—Downloadable from www.NationaalCoordinatorGroningen.nl

Korswagen PA, Rots JG (2020a) Monitoring and quantifying crack-based light damage in masonry walls with Digital Image Correlation. In: 1st international conference on structural damage modelling and assessment (SDMA). Gent, Belgium

Korswagen PA, Rots JG (2020b) Older clay masonry can be more earthquake-resistant than calcium-silicate masonry for light damage. In: 17th international brick and block masonry conference (IB2MaC). Krakow, Poland

Vermeltfoort R (1993) Deformation controlled tests in masonry shear walls. Part 2. Report No: TUE/BKO/93.08, EindhovenUniversity of Technology, Eindhoven, Netherlands, 1993 (in Dutch)

van Zijl G, Rots JG, Vermeltfoort A (n.d.) Modelling shear-compression in masonry. In: 9th Canadian masonry symposium